

Dynamics of breaking arches under a constant vibration

Bruno Guerrero^{1,*}, Celia Lozano^{1,2,**}, Iker Zuriguel^{1,***}, and Angel Garcimartín^{1,****}

¹Dpto. de Física y Mat. Apl., Fac. Ciencias, Univ. Navarra, 31080 Pamplona, Spain

²Max-Planck-Institut für Intelligente Systeme, 70569 Stuttgart, Germany

Abstract. Granular flow through an orifice can be suddenly halted by the formation of arches in the vicinity of the outlet, which are stable under the action of gravity. They may be broken when an external driving (for instance, vibration) is applied. With the aim of shedding light on the dynamics of arch destruction, we built an experiment consisting of a vertical two-dimensional silo filled with monodisperse beads, to which a constant vibration is applied. It was previously found that an important parameter to predict the robustness of the arch is the angle between consecutive beads. We focus on long-enduring arches and study the angles among the beads along time. We have found that in many cases the dynamics of the largest angle determines the breaking of the arch; it does not only determine where the “weakest link” is, but also the process that leads to the final destabilization. This is interesting because it can provide information about whether the flow will resume in a well-defined time or not, which is especially useful for industrial processes that have to constantly deal with the possible emergence of clogs.

1 Introduction

Clogging arches that stop the flow of grains at the exit orifice of a silo are a nuisance in industry, and they are at the same time a nice example of clogging in many other systems [1]. It is known that under a sustained vibration, arches can be shattered alleviating the problem [2–4]. In that scenario flow becomes intermittent, alternating between clogs and flow intervals. Then, in order to characterize the flow, it becomes necessary to understand both the clogging and unclogging processes. The first one has been widely studied since 2001 [5] observing that the clogging probability is constant over time yielding an exponential distribution of the flowing times [6–11]. The unclogging process, however, has shown temporal dependence and the distribution of breaking times is compatible with a power law decay [1, 2, 4]. The origin of this is still not fully understood but it could be related with aging, creeping motion or other complex slow dynamics [12]. Incidentally, let us mention that this power law decay of the unclogging times has been also observed in other systems such as colloids, sheep or pedestrians evacuating a room [1, 13, 14].

In previous works [4, 15], it was reported that the angle ϕ between adjacent beads of an arch (see Fig. 1) is an important variable to understand the unclogging process as it affects the robustness of the mechanical structure. In fact if the maximum angle in an arch ϕ_{max} was larger than 180° (that was called a defect) it was found a linear relationship

between ϕ_{max} and the vibration intensity at which arches break down [15].

Here we explore the dynamics of arches that collapse when they are submitted to an external vibration. For the vibration parameters used here, most of the arches collapse in a very short time. We select those that last longer than a certain threshold and break down before a temporal upper bound set beforehand (mainly imposed by the experimental constraints). In Fig. 2, we show an example of how much the beads have moved after 20 minutes of sustained vibration; it can also be appreciated how the arch balls move unevenly in space. This issue is important in determining how do arches evolve to resist the external forcing.

The paper is organized as follows, We initially summarize the experimental methods. In the following section we introduce the first results obtained. Finally, we make a few concluding remarks about the future research.

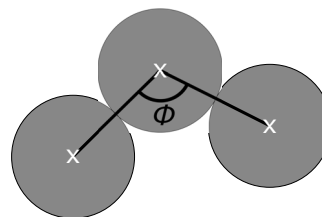


Figure 1. Sketch which illustrates the definition of the angle between adjacent beads ϕ . It is the inner angle formed between the straight lines connecting the center of a bead with the centers of the two adjacent beads, all of them belonging to the arch. The maximum angle ϕ in the arch is called ϕ_{max} .

* e-mail: bguerrero.3@alumni.unav.es

** e-mail: c.lozano@physik.uni-stuttgart.de

*** e-mail: iker@unav.es

**** e-mail: angel@unav.es

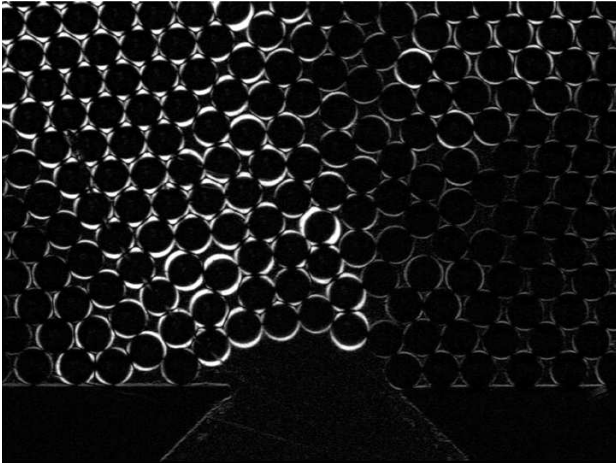


Figure 2. The subtraction of two images of an arch, one before and the other after enduring a sustained vibration for 20 minutes (bright zones correspond to displacements of the beads).

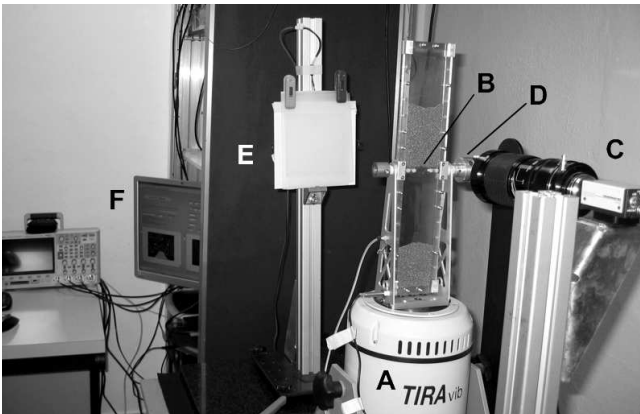


Figure 3. Photograph of the experimental setup: A, shaker; B, silo (the line points to the orifice); C: camera and lens; D: motor to rotate the silo; E: led lighting; F: devices and computer (a photograph of the arch is visible on the computer screen).

2 Experimental set-up and methods

The experimental set-up is the one used by Lozano *et al.* [4]. It consists of a two dimensional silo mounted on top of an electromagnetic shaker (see Fig. 3). The silo is filled with monodisperse steel beads that have a diameter of 1 mm. It has an orifice in the middle, and so an electric motor can turn the container to start anew with another run. A camera records the zone near the orifice, detecting the arches. The automated procedure starts with grains flowing through the orifice; when an arch is formed it is detected by a real time image analysis, the vibration is switched on and the image acquisition begins. The run stops when the arch breaks (or after 20 minutes of sustained vibration if the arch has not been shattered by that time).

The improvement and novelty needed for the present measurements is both in the image acquisition stage and in the image processing. In fact, we need as many images as possible for long periods. We have written an *ad-hoc*

software to perform this task. With it, we are able to collect snapshots with a standard video camera at a rate of nearly 25 frames per second (the camera rate) for long periods of time. It should be noted that once in a while the operating system flushes the buffer and a comparatively long time lapse (up to a few seconds) between two consecutive images is found; but this only happens occasionally after the experiment has run for many seconds, so this is not really important because it only affects the description at long times –when fast processes are not important. For short times, our temporal resolution is of about 0.05 s. The longest time span during which we register images is 20 minutes, so the dynamic range covers four orders of magnitude.

Images are time-stamped and stored in the hard disk, where they are processed at another stage. We have implemented a program for detecting the centres of the beads with subpixel resolution. It was inspired in a code written by M. Shattuck [16], in which the maxima of the convolution of a disk with the image provides the particles' centres (the disk size must be close to the size of the beads). With our code a resolution of 0.1 pixels is attained; a better resolution is feasible, but we did not go further as the stability of the silo during one run is about 1 micron (and 0.1 pixel corresponds to 2 microns). The position changes of the beads we track are typically two orders of magnitude bigger than this (see Fig. 2), so this resolution is enough for our purposes. Note that the height of the base can slightly shift up and down –this is barely visible in Fig. 2– due to the vibration; this item has been dealt with in the image processing stage.

3 Results

It was previously reported [4] that the time needed to break an arch (t_b) follows a probability distribution displaying a power law decay $P(t_b) \propto t_b^{-\alpha}$. Incidentally, this means that if the exponent α is smaller than two, the first moment of the distribution does not converge and the average breaking time $\langle t_b \rangle$ will depend on the size of the sample. It is usually more convenient to work with the complementary cumulative distribution function $P(T \geq t_b)$, because it is less noisy; note that the power law tail for the cumulative distribution has an exponent $\alpha + 1$.

Inspired by the fact that the force needed to break the arches is related to the maximum angle found within the arch at the beginning (when the vibration is switched on), we have sought a dependence between t_b and this ϕ_{max} . We have checked that the subpopulations of arches grouped by ϕ_{max} also have such distributions [4]. For each one of these classes, a power law tail can be fitted with an exponent that is different for each group (see Fig. 4). Groups of arches with a bigger ϕ_{max} display both, a shorter breaking time and a larger α . The fact that the distribution of t_b is to a great extent determined by ϕ_{max} at the moment of the arch formation underscores the notion that the bead associated to this angle will largely dominate the dynamics of the arch breaking.

Assuming that this is so, and taking into account that a larger ϕ_{max} leads to short-lived arches, one can further

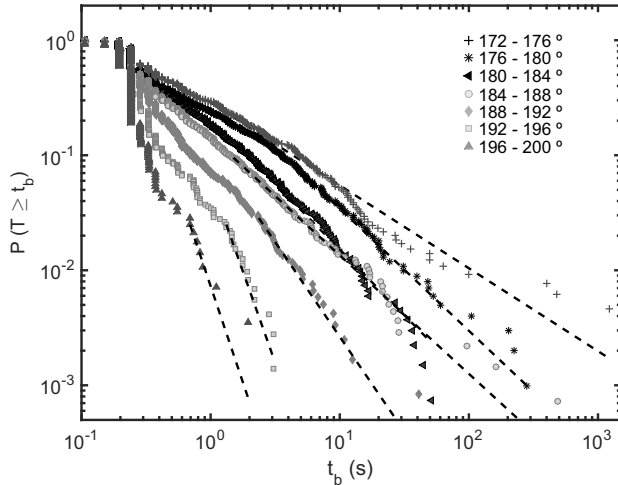


Figure 4. Complementary cumulative distribution function of the breaking times (sometimes also called survival function): it is the probability that an arch endures the vibration for a time equal or longer than t_b . Note the logarithmic scale. These data have been obtained for $R = 4.5 \text{ mm}$, $f = 100 \text{ Hz}$ and an acceleration of $2.6 g$. The power law tails have been fitted (*dashed lines*) using the method described in [17], giving the following exponents (from left, bigger angles, to right, small angles): $\alpha = 4.1, 4.1, 2.6, 2.05, 2.1, 2.1, 1.6$.

hypothesise that

$$\frac{d\phi}{dt} \propto \phi \quad (1)$$

(or alternatively, $d\phi/dt$ could be proportional to a growing function of ϕ , in which case Eq. 1 would be just a first approximation). If this equation is valid, the dynamics of ϕ_{max} will be the fastest. As changing the angle of one bead would affect the angle of other beads, it can be concluded that if the above statements hold, then the dynamics of the arch is *slaved* to that of the bead associated to ϕ_{max} .

Some previous unpublished observations that we carried out with a high speed camera suggest that indeed arches break in a way that could be described as explained above. In these inspections, we have seen that the bead starting with ϕ_{max} is usually the one that moves faster, and the last stages of the breaking process give something close to an exponential growth for ϕ vs. time. But only weak arches (with a big ϕ_{max}) were accessible to this survey, because the high speed camera is able to store just a short time span – a few seconds. These are usually the arches that have a big initial defect (a bead with a large ϕ_{max}), and consequently break after a short time span.

In the following we will consider the dynamics of long-lived arches. We have fixed the size of the exit orifice at 4.5 mm and recorded the formation of more than three thousand arches, as explained in Sect. 2. Once the arch was formed, the shaker was switched on, imparting the whole silo a constant sinusoidal vibration with a peak acceleration of $0.6 g$ (where g is the gravity acceleration) and a frequency of 105 Hz . Of all these arches, 174 (just over 5% of the total) withstood the vibration for more than

one minute and broke before 20 minutes; we selected these for the following analysis.

After recording the images, we measured the angles associated to each bead in the arch along time. As an example, in Fig. 5, we plot the evolution of the angles of the beads in two arches along time. The accuracy of ϕ attained with our measurements is $\pm 0.5^\circ$. Fig. 5 (a) depicts the case of an angle with 5 beads that breaks slightly after two minutes (just after the photograph shown in Fig. 5 (b)). The bead associated to ϕ_{max} is a defect ($\phi > 180^\circ$), and this angle increases monotonically during all the lifespan of the arch, as shown in Fig. 5 (c). Moreover, the arch breaks precisely there. Note also how $d\phi/dt$ grows bigger as ϕ increases. This is a good example of an arch amenable to be described with Eq. 1.

On the other hand, for the case displayed in Fig. 5 (d-f), the bead starting with ϕ_{max} is not the one where the arch finally breaks down; another bead with smaller ϕ overtakes it and governs the dynamics. Remark, however, that this bead had already begun as a defect, and it is not the only one; thus in this arch there is not a clearly dominant defect governing the dynamics of the whole structure.

It is noteworthy that among the selected 174 arches, 138 (representing 79%) broke at the bead with ϕ_{max} , and only 36 broke at a bead that was *not* the one sporting the maximum angle when the vibration was switched on. Of course, in these cases Eq. 1 does not hold (at least during the whole lifetime of the arch). Note that this is in agreement with the figures given in [15] which correspond to another kind of independent experiments.

The dynamics of the beads in the zone close to the arch (see Fig. 2) are also interesting. For example, although there is an ordered arrangement due to the 2D geometry (see Figs. 2 and 5), just over the arch this order seems to be smaller. We cannot use bidisperse beads to avoid this, but it would be interesting to study compaction in that zone. We know from numerical simulations that flow, stresses and local compaction does not change a lot if there is a small amount of polydispersity. Particle shape should not change a lot these results provided that the particles do not have flat faces.

This opens a new landscape to be explored, namely, how and why do some arches endure the vibration for a long time. For instance, how many of the beads where the arch breaks display the fastest dynamics? Do they all begin as a defect? Are the motions of *all* the beads correlated and effectively slaved to the fastest one? Many more data are needed to answer these questions, but the results shown here demonstrate that the analysis developed can be helpful to tackle them.

4 Conclusions

We have reported the first results of an experiment in which we can record and analyze the dynamics of long-lasting arches when submitted to an external vibration. We have shown how in many cases the initial “weakest link” (the bead with the maximum ϕ) may determine the dynamics of the whole arch. Moreover, it seems that at least in

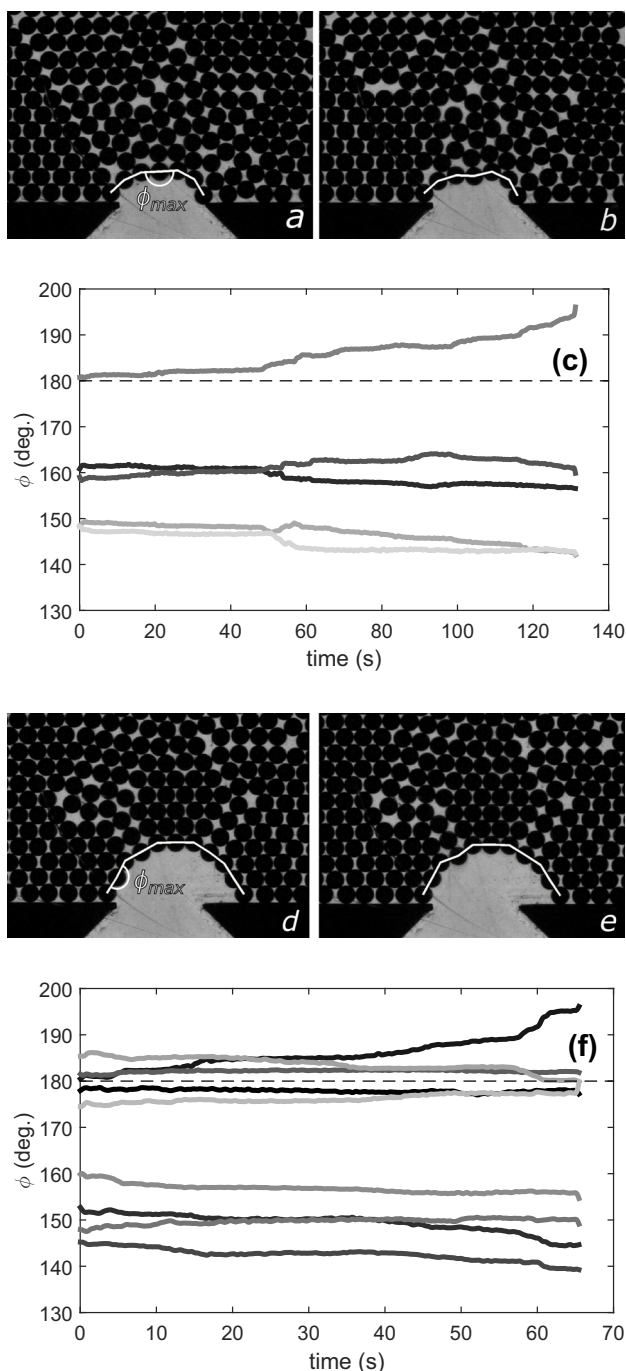


Figure 5. Evolution of the angles ϕ corresponding to the beads in an arch along of time. **(a)** An arch just formed, before the vibration begins. The maximum angle is indicated. Note that the base of the arch (the beads at the left and right ends) are not considered to belong to the arch. The white line joins the centers of the arch beads. **(b)** The last photograph of the arch before breaking. **(c)** The evolution of all the angles for the arch shown in (a) and (b). Here the dynamics is “slaved” to ϕ_{max} . **(d)** Another arch just formed, before the vibration begins. The maximum angle is indicated. **(e)** The last photograph of the arch in (d) before breaking. **(f)** The evolution of all the angles for the arch shown in (d) and (e). In this case, ϕ_{max} is not governing the dynamics. Remark that cases like the latter are much scarcer than the former. In plots (c) and (f), each shade corresponds to one bead, and the thickness of the lines are approximately equal to the experimental accuracy. The dashed horizontal line at $\phi = 180^\circ$ allows to identify defects.

some cases (see Fig. 5 (a-c)) the motion of the other beads in the arch may be correlated to the motion of the fastest one. In some other cases this is not so, and the dynamics of these arches is not trivial and is not governed by the biggest initial defect.

The analysis presented here may allow to identify whether long-lived arches are born with a special configuration, or whether they evolve to become more robust. And it can also be helpful to determine if certain kind of mechanisms (for instance, stick-slip) are present in the process.

Acknowledgements

We thank L.F. Urrea for technical help, and D. Maza and R. Cruz Hidalgo for discussions and comments. This work was funded by Ministerio de Economía y Competitividad (Spanish Government) through Project No. FIS2014-57325. BG also thanks Asociación de Amigos de la Universidad de Navarra for a grant.

References

- [1] I. Zuriguel *et al.*, *Sci. Rep.* **4**, 7324 (2014).
- [2] A. Janda *et al.*, *EPL* **87**, 24002 (2009).
- [3] C. Mankoc *et al.*, *Phys. Rev. E* **80**, 011309 (2009).
- [4] C. Lozano, I. Zuriguel, and A. Garcimartín, *Phys. Rev. E* **91**, 062203 (2015).
- [5] K. To *et al.*, *Phys. Rev. Lett.* **86**, 71 (2001).
- [6] I. Zuriguel *et al.*, *Phys. Rev. E* **68**, 030301 (R) (2003).
- [7] K. To, *Phys. Rev. E* **71**, 060301 (R) (2005).
- [8] J. Tang and R. P. Behringer, *Chaos* **21** 041107 (2011).
- [9] S. Tewari, M. Dichter, and B. Chakraborty, *Soft Matter* **9**, 5016 (2013).
- [10] L. Kondic, *Granular Matter* **16**, 235 (2014).
- [11] C. C. Thomas and D. J. Durian, *Phys. Rev. Lett.* **114**, 178001 (2015).
- [12] B. Blanc, J.-C. Géminard, and L. A. Pugnaloni, *Eur. Phys. J. E* **37**, 112 (2014).
- [13] J. M. Pastor *et al.* *Phys. Rev. E.* **92**, 062817 (2015).
- [14] A. Nicolas, S. Bouzat, and M. Kuperman, *Phys. Rev. E* **94**, 022313 (2016).
- [15] C. Lozano, G. Lumay, I. Zuriguel, R. C. Hidalgo, and A. Garcimartín, *Phys. Rev. Lett.* **109**, 068001 (2012).
- [16] M. D. Shattuck, “Particle tracking”, <http://gibbs.engr.ccnycunyu.edu/technical/Tracking/ChiTrack.php>
- [17] A. Clauset, C. R. Shalizi, and M. E. J. Newman, *SIAM Rev.* **51**, 661 (2009).